WP20–JRA1: Lidar and sunphotometer – Improved instruments, combined observations and integrated algorithms

Deliverable D20.7: Documentation on the inversion algorithm for combined sunphotometer and multiwavelength Raman lidar data

Objectives and overview

Latest advances in Raman lidar technology allow performing Raman observation not only at night but also at daytime. At the same time more and more lidar systems are being equipped with Raman channels. The most wide spread lidar systems perform backscatter measurements at wavelengths of the YAG laser (355, 532 and 1064 nm) together with Raman scattering by atmospheric nitrogen at 387 and 607 nm.

Raman scattering observations were introduced earlier in order to retrieve aerosol lidar ratio and vertical extinction profiles (Ansmann et al., 1990, 1992). Latest developments are focused on estimation of properties of cloud particles on the base of observations of Raman multiple scattering (Malinka, 2007).

The method of estimation of aerosol extinction from Raman sounding includes differentiation of logarithm of lidar signals ratio. In the presence of noise such solution of lidar equation relative to aerosol extinction becomes an ill-posed problem. This issue could be resolved only in special situations, at lower altitude resolution, with long accumulation time and only for the layers with high aerosol loading.

Standardised processing of lidar network observations requires a more sophisticated algorithm that allows searching for physical solutions and preserving high altitude resolution of the retrieved aerosol characteristics under situations with the presence of noise in Raman signals and low aerosol optical thicknesses. Such data could be treated using statistically optimized algorithms with use of adequate a priori constraints. The review of inversions techniques can be found in Turchin (1971) and Tarantolla (1987).

1 General description of the inversion algorithm

The algorithm for retrieval of optical and microphysical properties of atmospheric aerosols from combined sun-photometer and multi-wavelength Raman lidar could be divided into several independent modules with particular functions, whose interactions are minimized to straightforward exchange of limited set of parameters (see Fig. 1).

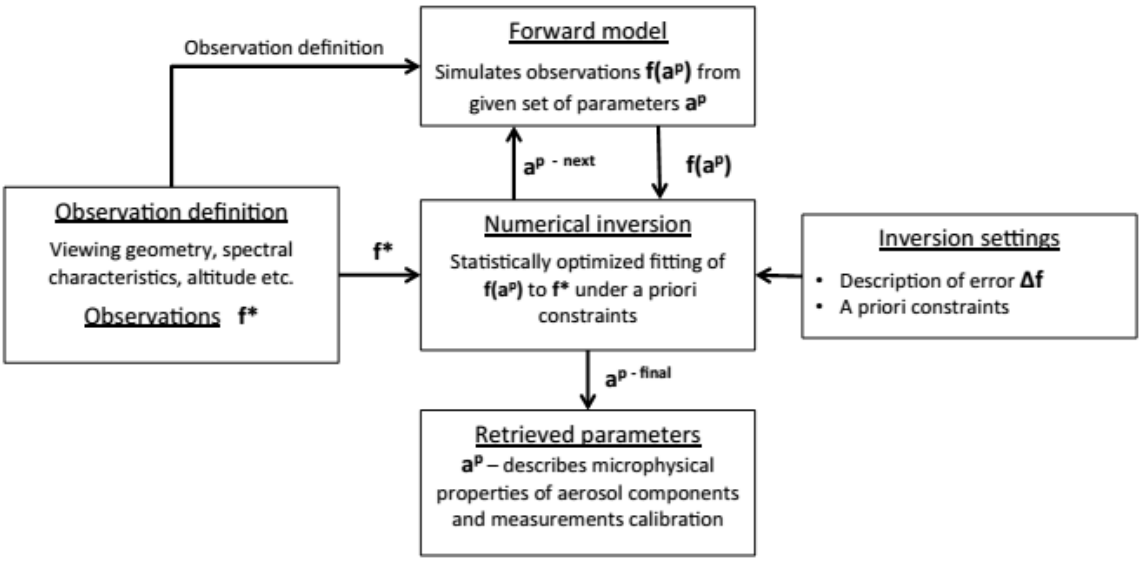

Figure 1. General structure of combined sun-photometer/Raman lidar retrieval algorithm.

The **forward model** of scattered radiances measured by complex AERONET and lidar observations contains four main components (as shown in Fig. 2):
• aerosol single scattering,
• aerosol optical properties vertical profiling,
• lidar equation and
• vector radiative transfer equation.

The modelling of **aerosol single-scattering** columnar optical properties has been implemented following the ideas employed in AERONET retrieval algorithm by Dubovik and King (2000) and Dubovik et al. (2002, 2006). This concept was developed to model the particles as a mixture of spherical and non-spherical aerosol components.

Simulation of sun-photometer measurements is implemented by the successive order of scattering **radiative transfer** code (Lenoble et al., 2007). The code provides full information about the atmospheric radiation field including I and Q, U components of the Stokes vector under the assumption of the plane parallel atmosphere. The developed version of successive order of scattering radiative transfer code allows calculations of atmospheric radiances for the aerosol composed by several components (k).

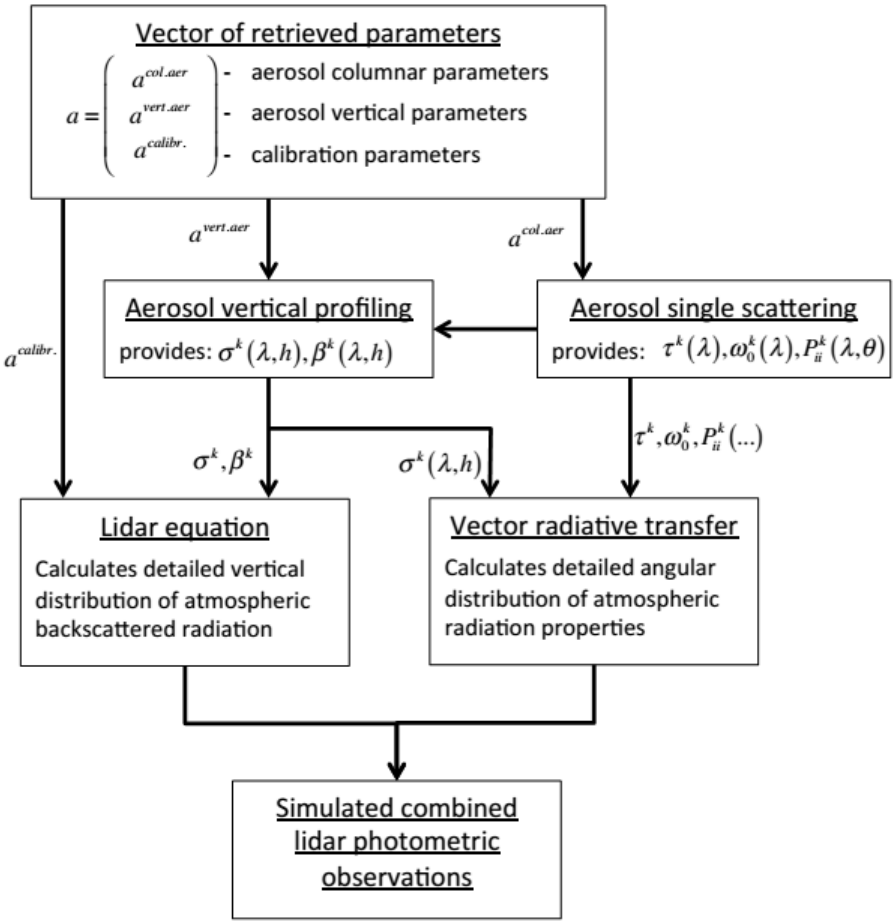

Figure 2. General scheme of forward modelling of combined sun-photometer/multi-wavelength Raman lidar observations.

Each aerosol component is described by altitude independent phase matrix $P_{ij}^k(\lambda,\theta)$ and single-scattering albedo $\omega_0^k(\lambda)$ determined on the base of microphysical model of atmospheric aerosol together with the vertical profile of aerosol concentrations $c_k(h)$ which determines the vertical variability of spectral extinction $\sigma_a^k(\lambda,h)$ of atmospheric aerosol. Correspondingly, only set of parameters describing aerosol microphysics and is directly included in the set of retrieved parameters. Specifically, the vertically invariant is driven by: the shape of the size distribution $dV(r_i)/d\ln r$; the real $n_k(\lambda)$ and imaginary $\kappa_k(\lambda)$ parts of the complex refractive index; and the fraction of the spherical particles C_{sph}. For the convenience, the algorithm deals with normalized functional $c_k(h)$, which shows the vertical partitioning of integral characteristics such as aerosol concentration and extinction.

Since lidar measurements don't cover all atmosphere altitudes ($h_{BOA} < h < h_{TOA}$) and have upper and lower limits h_{min} and h_{max} correspondingly. Therefore, vertical profile of aerosol distribution is extrapolated:

$$c_k(h) = \begin{cases} c_k(h_{min}), h_{BOA} < h \le h_{min} \\ \sum_{i=1}^{N_h} c_k(h_{min}) D(h_i), h_{min} < h < h_{max}, \\ c_k(h_{max}) \exp(-\alpha h), h_{max} < h \le h_{TOA} \end{cases} \quad (1)$$

where α is chosen from the following considerations: $\exp(-\alpha h_{TOA}) \to 0$.

Vertical profiling of aerosol extinction coefficient is retrieved by the following equation:

$$\sigma_a^k(\lambda, h) = \tau_a^k(\lambda) c_k(h). \quad (2)$$

Lidar ratio is calculated from the columnar aerosol optical properties:

$$S_a^k(\lambda) = \frac{4\pi}{\omega_0^k(\lambda) P_{11}^k(\lambda, 180°)}. \quad (3)$$

Therefore aerosol backscatter coefficient is defined as follows:

$$\beta_a^k(\lambda, h) = \frac{1}{4\pi}\left(\tau_a^k(\lambda) c_k(h) \omega_0^k(\lambda) P_{11}^k(\lambda, 180°)\right). \quad (4)$$

The following **lidar equations** are used to model the attenuated backscatter provided by multi-wavelength Raman lidar (Chaikovsky et al., 2006):

$$L_e(\lambda, h) = A(\lambda)\left(\beta_a^f(\lambda, h) + \beta_a^c(\lambda, h) + \beta_m^e(\lambda, h)\right) \exp\left(2\left(\int_h^{h_{ref}} \sigma_a^f(\lambda, h) + \sigma_a^c(\lambda, h) + \sigma_m^e(\lambda, h)\right) dh'\right) \quad (5)$$

$$L_R(\lambda_R, h) = A(\lambda_R)\beta_m^e(\lambda, h) \exp\left(\int_h^{h_{ref}} \left(\left(\sigma_a^f(\lambda, h) + \sigma_a^c(\lambda, h)\right) + \left(\sigma_a^f(\lambda_R, h) + \sigma_a^c(\lambda_R, h)\right)\right) dh'\right), \quad (6)$$

where β_m^e denotes given elastic molecular backscatter, A is retrieved lidar calibration coefficient, indices *f* and *c* denote fine and coarse aerosol fractions, λ_R is the Raman shifted wavelength and h_{ref} is the reference altitude, used for lidar calibration (Russell et al., 1979).

The purpose of numerical inversion is to retrieve the vector describing microphysical properties of the atmospheric aerosol:

$$a = \begin{pmatrix} a_v \\ a_n \\ a_k \\ a_{sph} \\ a_h \\ a_A \end{pmatrix}, \quad (7)$$

where $a_v, a_n, a_k, a_{sph}, a_h, a_A$ denote the components of the vector of aerosol properties a, corresponding to size distribution, real and imaginary part of refractive index, fraction of the spherical particles, vertical profiles of aerosol concentration and lidar calibration coefficient *A*. All of the parameters listed above describing microphysical state of the aerosol in the atmosphere, except for the lidar calibration parameters, consist of two subsets of parameters, each describing independent aerosol component, corresponding to fine and coarse aerosol mode:

$$a_{\dots} = \begin{pmatrix} a_{\dots}^f \\ a_{\dots}^c \end{pmatrix}.$$

Inversion is considered as a multi-term Least Squares Method (LSM) that solves the following system of equations (Dubovik and King, 2000; Dubovik et al., 2011):

$$\begin{cases} f^* = f(a) + \Delta f \\ 0^* = (\Delta a)^* = Sa + \Delta(\Delta a), \\ a^* = a + \Delta a^* \end{cases} \quad (8)$$

where f^* is a vector of the combined measurements, Δf is a vector of measurement uncertainties and a is a vector of unknowns.

The second term represents the a priori smoothness assumptions used to constrain the variability of size distribution, vertical concentration and spectral dependencies of the real and imaginary parts of the refractive index. The matrix *S* includes the coefficients for calculating *m*-th differences (numerical equivalent of the derivatives) of $dV(r_i)/d\ln r$, $c_k(h)$, $n_k(\lambda)$ and $\kappa_k(\lambda)$; 0^* is the vector of zeros and $\Delta(\Delta a)$ is the vector of the uncertainties characterizing the deviations of the differences from the zeros. The third part includes the vector of a priori estimates a^* and Δa^* is the vector of the uncertainties in a priori estimates. The errors Δf, $\Delta(\Delta a)$, and Δa^* are assumed to be normally distributed.

According to the multi-term LSM concept, the solution for the Eq. (8) corresponds to the minimum of the following quadratic form:

$$\begin{aligned}\Psi(a^p) &= \Psi_{\mathrm{f}}(a^p) + \Psi_{\Delta}(a^p) + \Psi_{\mathrm{a}}(a^p) \\ &= \frac{1}{2}\Big((f(a^p) - f^*)^T W_f^{-1}(f(a^p) - f^*) + \gamma_{\Delta}(a^p)^T \Omega a^p \\ &+ \gamma_a(a^p - a^*)^T W_a^{-1}(a^p - a^*)\Big).\end{aligned}$$

The minimum is obtained by the iterative procedure:

$$a^{p+1} = a^p - t_p \Delta a^p, \tag{10}$$

where a^p is the p-th the solution of so called normal system:

$$A_p \Delta a^p = \nabla\Psi(a^p), \tag{11}$$

where A_p is the Fisher Matrix and the right side and represents the gradient $\nabla\Psi(a^p)$:

$$\nabla\Psi(a^p) = \mathrm{K_p^T W_f^{-1}\Delta f^p} + \gamma_{\Delta}\Omega\mathrm{a^p} + \gamma_{\mathrm{a}}\mathrm{W_a^{-1}(a^p - a^*)}, \tag{12}$$

$$A_p = \mathrm{K_p^T W_f^{-1} K_p} + \gamma_{\Delta}\Omega + \gamma_{\mathrm{a}}\mathrm{W_a^{-1}}, \tag{13}$$

where $\Delta f = f(a^p) - f^*$ and K_p is the Jacobi matrix of the first derivative $\frac{\partial f(a^p)}{\partial a_i}$ and W are the weighting matrices, defined by Dubovik and King (2000) as follows:

$$W_{\dots} = \frac{C_{\dots}}{\varepsilon_{\dots}}, \tag{14}$$

where $\varepsilon_{\dots}^2 = \{C_{\dots}\}_{11}$ are the first diagonal elements of the corresponding covariance matrices $C_{\dots}$ and $\gamma_{\dots}$ are Lagrange multipliers, defined by Dubovik (2004):

$$\gamma_{\dots} = \frac{N_f \varepsilon_f^2}{N_{\dots}\varepsilon_{\dots}^2}, \tag{15}$$

where $N_{\dots}$ are the sizes of corresponding vectors.

The vector of combined sun-photometer and multi-wavelength Raman lidar measurement could be considered as consistent of seven components, representing independent measurements with different level of accuracies:

$$f^* = \begin{pmatrix} f_\theta \\ f_\tau \\ f_{\beta_1} \\ f_{\beta_2} \\ f_{\beta_3} \\ f_{\alpha_1} \\ f_{\alpha_2} \end{pmatrix}, \tag{16}$$

where index θ denotes sun and sky radiances, τ stands for optical thickness, $\beta_{\dots}$ is for elastic lidar measurements at three different wavelengths, and $\alpha_{\dots}$ is for Raman lidar measurements. These measurements are made with different accuracy and under assumption that observations are uncorrelated and provide equally accurate data (i.e. weighting matrices are equal to unity matrices) covariance matrices will have the following array structure:

$$C_f = \begin{pmatrix} \varepsilon_\theta^2 I & 0 & 0 & & 0 & 0 & 0 & 0 & \\ 0 & \varepsilon_\tau^2 I & 0 & & 0 & 0 & 0 & 0 & \\ 0 & 0 & \varepsilon_{\beta_1}^2 I & & 0 & 0 & 0 & 0 & \\ & 0 & 0 & 0 & \varepsilon_{\beta_2}^2 I & 0 & 0 & 0 & \\ & 0 & 0 & 0 & 0 & \varepsilon_{\beta_3}^2 I & 0 & 0 & \\ & 0 & 0 & 0 & 0 & 0 & \varepsilon_{\alpha_1}^2 I & 0 & \\ & 0 & 0 & 0 & 0 & 0 & 0 & \varepsilon_{\alpha_2}^2 I & \end{pmatrix}, \tag{17}$$

The **a priori constraints** are applied in the developed algorithm on several different components of the vector a differently, same as in previous approaches (Dubovik and King, 2000; Dubovik, 2004; Dubovik et al., 2011). Two types of the constraints could be applied both together and separately: smoothness constraints, which limit the variation of the retrieved parameters and direct constraints, which limit their value. Considering the Eq. (7) the smoothness matrix will have the following form:

$$Sa = \begin{pmatrix} S_v & 0 & 0 & 0 & 0 & 0 \\ 0 & S_n & 0 & 0 & 0 & 0 \\ 0 & 0 & S_\kappa & 0 & 0 & 0 \\ 0 & 0 & 0 & 0 & 0 & 0 \\ 0 & 0 & 0 & 0 & S_h & 0 \\ 0 & 0 & 0 & 0 & 0 & 0 \end{pmatrix} \begin{pmatrix} a_v \\ a_n \\ a_k \\ a_{sph} \\ a_h \\ a_A \end{pmatrix}, \tag{18}$$

The correspondent matrices $S_{\dots}$ have different dimension and represent differences of different order (3 for size distribution, 1 for real part of complex refractive index and 2 for imaginary part of complex refractive index and for vertical profile of aerosol concentration). The lines corresponding to a_{sph} and A contain only zeros because no smoothness constraints are applied on them.

Direct application of a priori constraints on the values of the retrieved vector could be useful in a situation when the sun-photometer data was already inverted therefore providing estimations on aerosol columnar size distribution, complex refractive index and spherical particles faction:

$$a^* = \begin{pmatrix} a_v^* \\ a_n^* \\ a_\kappa^* \\ a_{sph}^* \\ 0 \\ 0 \end{pmatrix}. \tag{19}$$

In such situation the corresponding covariance, smothering and weighting matrices will have the following forms:

$$C_f = \begin{pmatrix} \varepsilon_{\beta_1}^2 I & 0 & 0 & 0 & 0 \\ 0 & \varepsilon_{\beta_2}^2 I & 0 & 0 & 0 \\ 0 & 0 & \varepsilon_{\beta_3}^2 I & 0 & 0 \\ 0 & 0 & 0 & \varepsilon_{\alpha_1}^2 I & 0 \\ 0 & 0 & 0 & 0 & \varepsilon_{\alpha_1}^2 I \end{pmatrix}, \quad (20)$$

$$W_a = \begin{pmatrix} 1 & 0 & 0 & 0 & 0 & 0 \\ 0 & 1 & 0 & 0 & 0 & 0 \\ 0 & 0 & 1 & 0 & 0 & 0 \\ 0 & 0 & 0 & 1 & 0 & 0 \\ 0 & 0 & 0 & 0 & 0 & 0 \\ 0 & 0 & 0 & 0 & 0 & 0 \end{pmatrix}, \quad (21)$$

$$Sa = \begin{pmatrix} 0 & 0 & 0 & 0 & 0 & 0 \\ 0 & 0 & 0 & 0 & 0 & 0 \\ 0 & 0 & 0 & 0 & 0 & 0 \\ 0 & 0 & 0 & 0 & 0 & 0 \\ 0 & 0 & 0 & 0 & S_h & 0 \\ 0 & 0 & 0 & 0 & 0 & 0 \end{pmatrix} \begin{pmatrix} a_v \\ a_n \\ a_k \\ a_{sph} \\ a_h \\ a_A \end{pmatrix}. \quad (22)$$

The retrieval with the direct application of a priori constraints that were retrieved previously through the inversion of sun-photometer data could be considered as a “sequential” inversion, in a contrary to a “simultaneous” or “full” inversion when lidar and sun-photometer observations are processed simultaneously. In terms of “sequential” inversion adding the “lidar stage” allows differentiation of aerosol columnar properties over the altitude by providing information on aerosol vertical variability. At the same time adding Raman measurements to elastic backscatter measurements provides additional information on vertical variability of aerosol optical properties, including extinction and lidar ratio.

Compared to the “simultaneous” inversion, the “sequent” one uses a simpler aerosol model, distinguishing only vertical distribution of aerosol concentrations between fine and coarse modes. However, such model requires a much lower amount of regularisation parameters and a priori restrictions than a sophisticated model that allows full distinction between fine and coarse aerosol particles including complex refractive index, which is used in “parallel” inversion procedure. Lower amount of regularisation parameters makes it easier to get stable retrievals.

The “sequent” inversion of combined observations of multi-wavelength Raman lidar and sun-photometer was developed as an optional block of LiRIC inversion code, and allows application of additional constraints on aerosol lidar ratio, providing more accurate estimations compared to inversions including only sun-photometer and elastic lidar data.

2 Sequential algorithm for processing combined Raman and radiometer data

In the frame of sequential approach to solving problem of processing combined multi-wavelength lidar/radiometer data the columnar optical characteristics of aerosol model are obtained from radiometer data and are fixed as a priori parameters for sequential retrieving of altitude distribution of aerosol characteristics. With regard to processing data of Raman measurements, a value of AOT (or averaged aerosol lidar ratio) can be used as effective regularization factor.

The second specific of sequential approach is the possibility to develop an inversion algorithm for processing Raman lidar data as a separate procedure concerning the calculation of aerosol mode concentrations. Two parameters determine optical features of aerosol layer at the wavelength λ in the sequential algorithm:

- normalized aerosol backscatter coefficient at the wavelength :

$$\theta(\lambda,h)=\frac{\beta_a^e(\lambda,h)}{\beta_m^e(\lambda,h)} \tag{23}$$

- and aerosol lidar ratio:

$$S_a(\lambda,h)=\frac{\sigma_a^e(\lambda,h)}{\beta_a^e(\lambda,h)} \tag{24}$$

The variation of atmospheric parameters $\theta(h)$ and $S_a(h)$ is much smaller than of $\sigma_a^e(h)$ and $\beta_a^e(h)$. With small changes of the aerosol microstructure, the parameter $S_a(h)$ remains close to a constant value, while $\sigma_{a,e}(z)$ may vary considerably. Smaller variability of new variables allows more efficient application of the smoothness constraints in the retrieval procedure.

Two normalized and corrected lidar signals compose the input data files:

- Elastic signal

$$L_1^*(\lambda_1,h)=\frac{P_1(\lambda_1,h)h^2\exp(-2(\tau_{1,m}(\lambda_1,h,h_{ref}))}{P_1(\lambda_1,h_{ref})h_{ref}^2}R_1(\lambda_1,h_{ref}), \tag{25}$$

- Raman signal

$$L_2^*(\lambda_2,h)=\frac{P_2(\lambda_2,h)h^2\exp(-\tau_{1,m}(\lambda_2,h,h_{ref})-\tau_{2,m}(\lambda_2,h,h_{ref}))}{P_2(\lambda_2,h_{ref})h_{ref}^2}q_2, \tag{26}$$

where $P_1(\lambda_1,h)$ and $P_2(\lambda_2,h)$ are elastic and Raman lidar signals at the wavelengths λ_1 and λ_2, correspondingly; $\tau_{1,m}(\lambda_1,h,h_{ref})$ — optical molecular thickness of the layer between the levels h and h_{ref}; h_{ref} — altitude of the reference point; $R_{1,N}=R_1(z_r)=\left(\theta(z_N,\lambda_1)+1\right)$ - backscatter ratio in the reference point; q_2 — normalization coefficient.

The forward model for aerosol model defined by parameters (23) and (24) can be written as:

$$L_1^*(h)=L_1\left(\theta(h),\gamma(z_i)\right)+\mathbf{\Delta}_{L,1}, \tag{27}$$

$$L_2^*(h)=L_2\left(\theta(h),\gamma(h)\right)+\mathbf{\Delta}_{L,2}, \tag{28}$$

where

$$L_1\left(\theta_1(h),S_{1,,a}(h)\right)=\frac{\beta^e_{1,m}(h_{ref})(\theta(h)+1)}{\beta^e_{1,m}(h_{ref})}\exp\left[-2\int_{h_{ref}}^{h}S_{1,,a}(h)\beta^e_{1,m}(h)\theta_1(h)dh\right], \quad (29)$$

$$L_2\left(\theta(h),S_{2,a}(h)\right)=\frac{\beta^e_{1,m}(h)}{\beta^e_{1,m}(h_{ref})}\exp\left[-\int_{h_{ref}}^{h}(S_{1,a}\beta_{1,a}(h)+S_{2,a}\beta_{2,a}(h))dh\right], \quad (30)$$

$\beta^e_{j,m}$, $\beta_{j,a}$, $S_{j,a}$ θ_1 means $\beta^e_m(\lambda_j)$, $\beta_a(\lambda_j)$, $S_a(\lambda_j)$, $\theta(\lambda_1)$, respectively.

Supposing the ratio of extinction coefficient at the wavelength λ_1 and λ_2 to be constant

$$\eta=\frac{S_{2,a}(h)\beta^e_{2,a}(h)}{S_{1,a}(h)\beta^e_{1,a}(h)}\equiv const, \quad (31)$$

one can retrieve:

$$L_2\left(\theta(h),S_{2,a}(h)\right)=\frac{\beta^e_{1,m}(h)}{\beta^e_{1,m}(h_{ref})}\exp\left[-(1+\eta)\int_{h_{ref}}^{h}S_{1,a}(h)\theta(h)\beta^e_{1,m}(h)dh\right], \quad (32)$$

where $\theta(h)\equiv\theta_1(h)$ and $S_a(h)\equiv S_{1,a}(h)$.

Retrieving of aerosol parameters $\theta(h)$ and $S_a(h)$ provides by minimization of the functional

$$\Psi\ \left(L^*_1,\mathbf{L}^*_2,S_a,\theta,R_1,q_2\right)=\Psi_1+\Psi_2+\Psi_3+\Psi_4+\Psi_5, \quad (33)$$

where

$$\Psi_1==\sum_{n=0}^{N}\frac{k_1^2}{\Omega_{L_1,n}}\left(L^*_{1,n}-L_1\left(\theta(y_n),S_a(h_n)\right)\right)^2, \quad (34)$$

$$\Psi_2==\sum_{n=0}^{N}\frac{k_2^2}{\Omega_{L2,n}}\left(L^*_{2,n}-L_2\left(\theta(h_n),S_a(h_n)\right)\right)^2, \quad (35)$$

$$\Psi_3\left(\theta\right)=\sum_{n=0}^{n=N}\frac{d_1^2}{\left|\Delta h\right|^3}\left(2\theta(h_{n)})-\theta(h_{n-1)})-\theta(h_{n+1)})\right)^2, \quad (36)$$

$$\Psi_4\left(\theta\right)=\sum_{n=0}^{n=N}\frac{d_2^2}{\left|\Delta h\right|^3}\left(2S_a(h_{n)})-S_a(h_{n-1)})-S_a(h_{n+1)})\right)^2, \quad (37)$$

$$\Psi_5\left(\theta\right)=\sum_{n=N_1}^{n=N_2}\frac{d_3^2}{\left|\Delta z_n\right|}\left(S_a(z_{n)})-S_{a,0}\right)^2, \quad (38)$$

where $\Omega_{L_1,n}$ and $\Omega_{L2,n}$ are covariance matrixes of error vectors $\mathbf{\Delta}_{L,1}$ and $\mathbf{\Delta}_{L,2}$ respectively, in equations (5) and (6); k_x and d_x are the weight coefficients. The functions Ψ_1 and Ψ_2 are the differences between measured and calculated lidar signal for given parameters $\theta(h)$ and $S_a(h)$. Equations (26) and (27) provide constraints on smoothness of the parameters $\theta(h)$ and $S_a(h)$.

Functional Ψ_2 restricts the deviation of the retrieved $S_a(h)$ from value of averaged lidar ratio $S_{a,0}$ obtained from radiometer measurements. If radiometer data are unavailable, estimation of $S_{a,0}$ is carried out at the preliminary stage of the inversion from Raman and backscatter lidar signals.

3 Development of LiRIC program package for processing combined multi-wavelength Raman and radiometer data

Additional program modules have been developed for processing data of combined multi-wavelength Raman and radiometer data. The structure of the second version of improved program package LiRIC is shown in the Figure 3. The second version of LiRIC includes three program modules for retrieving profiles of aerosol mode concentrations ("**ConcentRetriever",** described in Deliverable WP20/D20.4), extinction/lidar ratio ("**RamanRetriever")** and depolarization ratio ("**PolarizRetriever"**). The new special "**Inversion settings, Error modeling"** module generates a set of input data files adding white noise and amplitude distortion to the initial data to provide error sensitivity analysis.

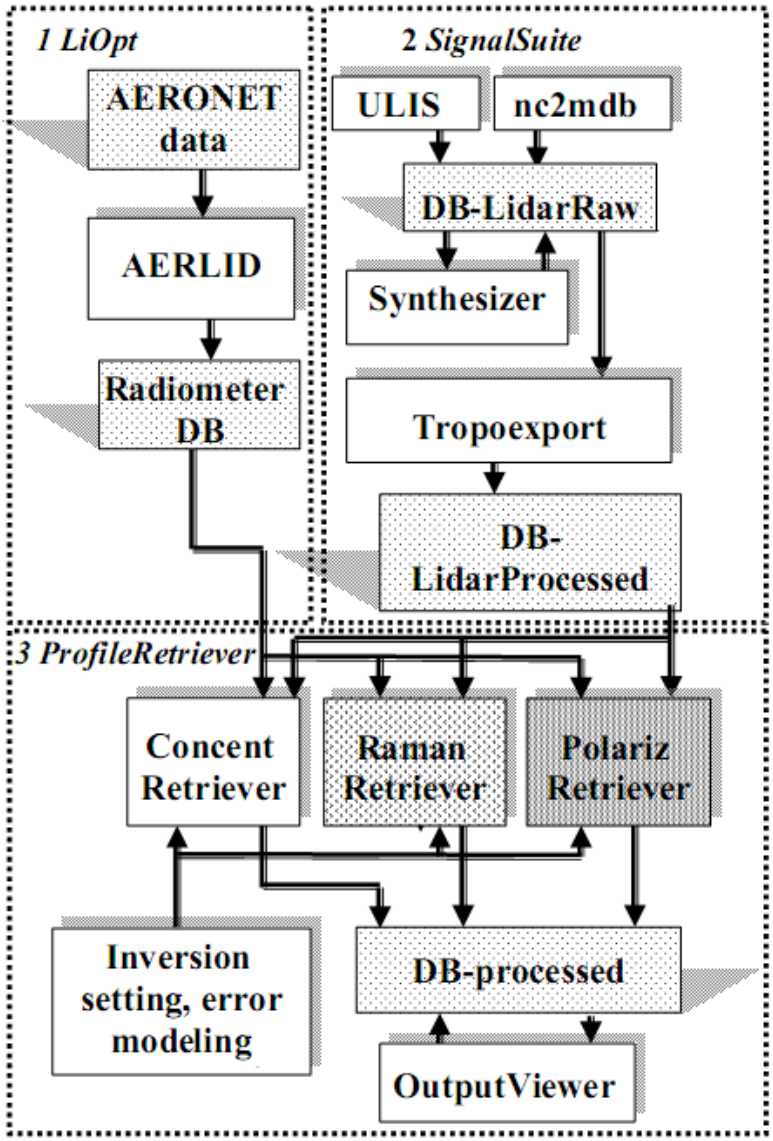

Figure 3. Structure of the second version of LiRIC program package. Current status of retrieving modules: ***ConcentRetriever*** *is in operational mode,* ***RamanRetriever*** *is in a test mode,* ***PolarizRetriever*** *is under development.*

4 Verifying LiRIC program package in intercomparison experiment EARLI09

Program modules of LiRIC have been tested by comparison of the results of the processing of multi-wavelength Raman data received by different teams in the frame of intercomparison experiment EARLI09, which was held in May 2009 at Leibniz Institute for Tropospheric Research in Leipzig, Germany. The comparison of the retrieved aerosol optical parameters from lidar data measured by lidars of Institute of Physics, Minsk and Leibniz Institute for Tropospheric Research, Leipzig at 21:04–22:55 on the 25th of May 2009 are shown in Figs. 4–6. Figures 4–6 show backscatter and extinction coefficients together with lidar ratio profiles at the wavelengths 355 and 532 nm, as well as standard deviation of these characteristics retrieved from the data provided by two lidars. Error estimations were made by simulation of the disturbed input data using error modelling module of LiRIC package. Profiles of the aerosol optical parameters show good agreement in structure and magnitude over the troposphere except for the lower boundary of the sounding range. The relative deviations are increased only when values of aerosol concentration become negligible that, most probably, is a result of uncertainty of lidar geometrical factor.

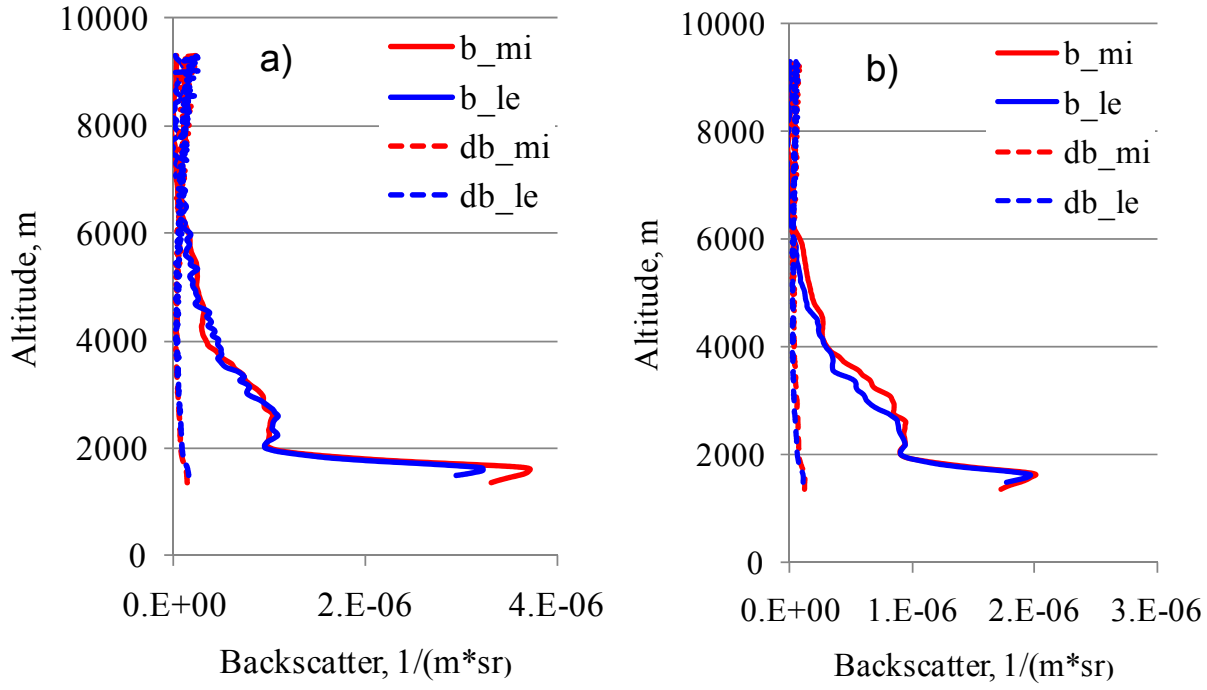

Figure 4. Backscatter coefficient (b_xx) and standard deviation (db_xx) profiles, measured by Minsk (_mi) and IFT Leipzig (_le) lidar at the wavelength 355 nm (a) and 532 nm (b), 21:04 – 22:55, 25 May, 2009, Leipzig, Germany.

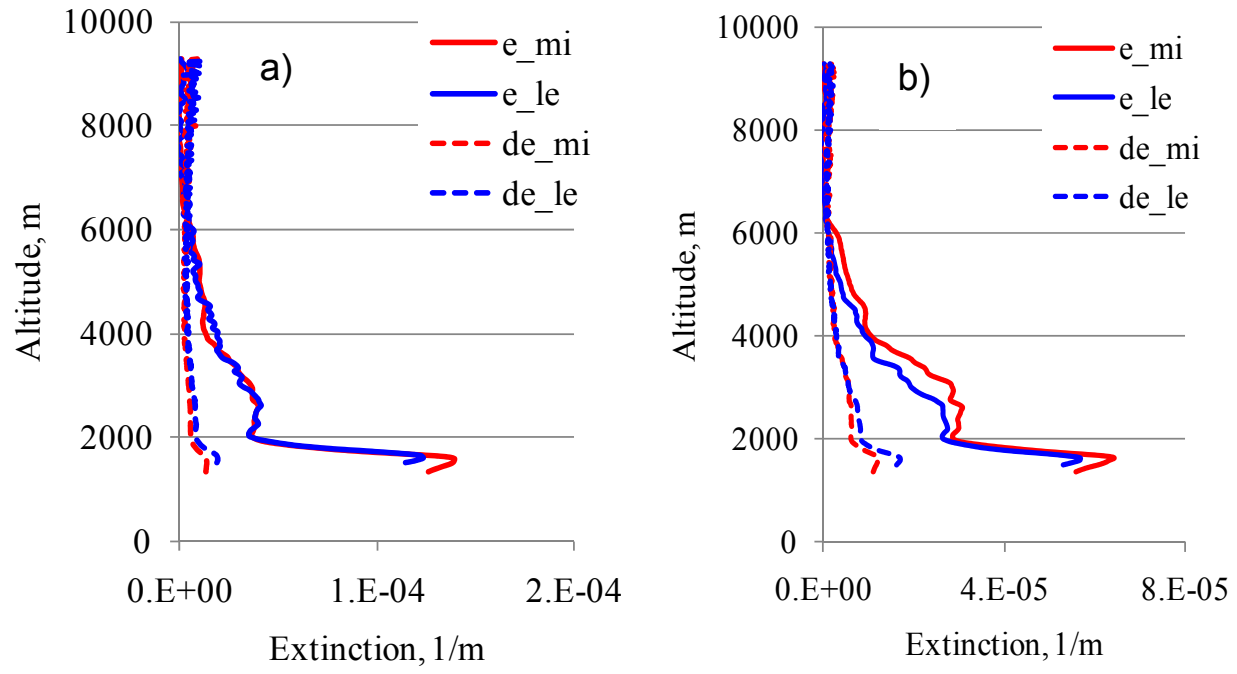

Figure 5. Extinction coefficient (e_xx) and standard deviation (de_xx) profiles, measured by Minsk (_mi) and IFT Leipzig (_le) lidar at the wavelength 355 nm (a) and 532 nm (b), 21:04 – 22:55, 25 May, 2009, Leipzig, Germany.

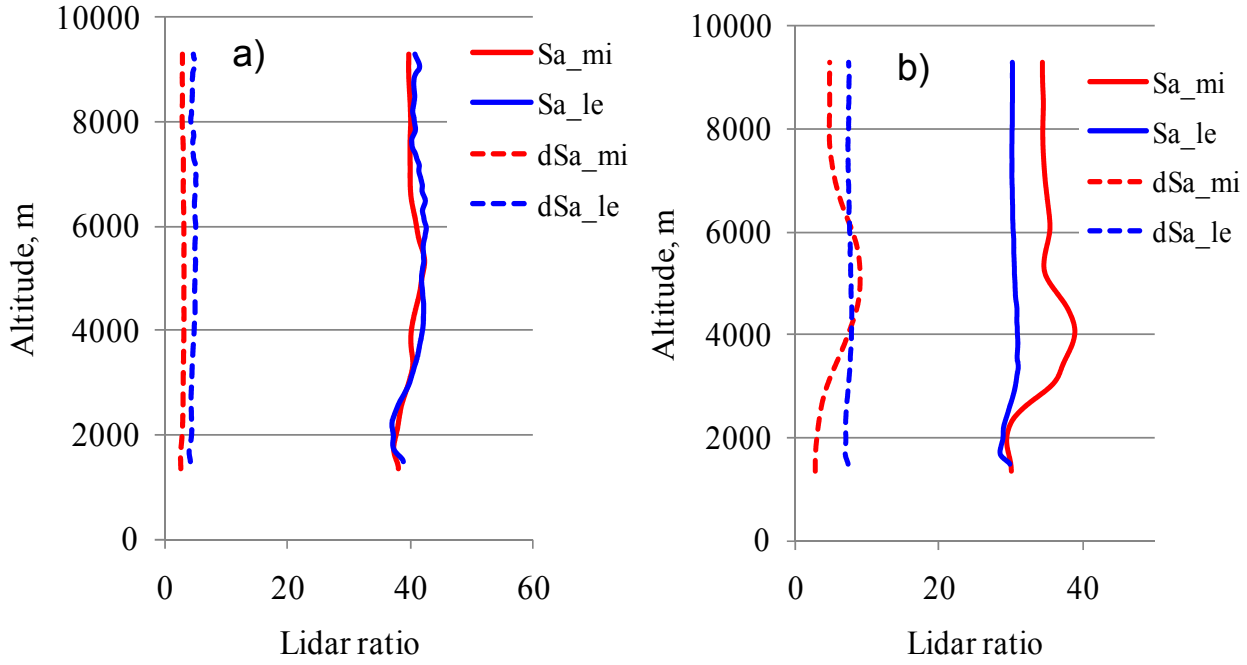

Figure 6. Lidar ratio (Sa_xx) and standard deviation (dSa_xx) profiles, measured by Minsk (_mi) and IFT Leipzig (_le) lidar at the wavelength 355 nm (a) and 532 nm (b), 21:04 – 22:55, 25 May, 2009, Leipzig, Germany.

References

Ansmann, A., Riebesell, M., and Weitkamp, C: Measurement of atmospheric aerosol extinction profiles with a Raman lidar, Opt. Lett., 15, 746–748, 1990.

Dubovik, O., and King, M.: A flexible inversion algorithm for retrieval of aerosol optical properties from Sun and sky radiance measurements, Journal of Geophysical Research, 105, 20 673–20 696, 2000.

Dubovik, O.: Optimization of Numerical Inversion in Photopolarimetric Remote Sensing, in: Photopolarimetry in Remote Sensing, edited by Videen, G., Yatskiv, Y. and Mishchenko, M., pp. 65–106, Kluwer Academic Publishers, Dordrecht, The Netherlands, 2004.

Dubovik, O., Holben, B. N., Lapyonok, T., Sinyuk, A., Mishchenko, M. I., Yang, P., and Slutsker, I.: Non-spherical aerosol retrieval method employing light scattering by spheroids, Geophysical Research Letters, 29, doi:10.1029/2001GL014506, 2002.

Dubovik, O., Sinyuk, A., Lapyonok, T., Holben, B. N., Mishchenko, M., Yang, P., Eck, T. F., Volten, H., Munoz, O., Veihelmann, B., van der Zande, W. J., Leon, J.-F., Sorokin, M., and Slutsker, I.: Application of spheroid models to account for aerosol particle nonsphericity in remote sensing of desert dust, Journal of Geophysical Research, 111, doi:10.1029/2005JD006619, 2006.

Dubovik, O., Herman, M., Holdak, A., Lapyonok, T., Tanré, D., Deuzé, J.-L., Ducos, F., Sinyuk, A., and Lopatin, A.: Statistically optimized inversion algorithm for enhanced retrieval of aerosol properties from spectral multi-angle polarimetric satellite observations, Atmospheric Measurement Techniques, 975–1018, 2011.

Chaikovsky, A., Bril, A., Denisov, S., and Balashevich, N.: Algorithms and software for lidar data processing in CIS-LiNet, in: Reviewed and Revised Papers Presented at the 23rd International Laser Radar Conference, 24–28 July 2006, Nara, Japan, edited by Chikao Nagasava, N. S., pp. 667–670, 2006.

Malinka A.: Raman lidar remote sensing of geophysical media, Light Scattering Reviews 2, Remote sensing and inverse problems, A. Kokhanovsky ed. – Berlin: Springer, 2007, pp. 125–155.

Russell, P. B., Swissler, T. J., and McCormick, M. P.: Methodology for error analysis and simulation of lidar aerosol measurements, Applied Optics, 18, 3783–3797, 1979.

Turchin, V.F., Kozlov, V.P., and Malkevich, M.S.: The use of mathematical-statistics methods in the solution of incorrectly posed problems, Sov. Phys. Usp., 13, 681–703, 1971.

Tarantola, A.: Inverse Problem Theory: Methods for Data Fitting and Model Parameter Estimation, Elsevier, Amsterdam, 1987, 614 pp.